

Unified description of floppy and rigid rotating Wigner molecules formed in quantum dots

Constantine Yannouleas and Uzi Landman

School of Physics, Georgia Institute of Technology, Atlanta, Georgia 30332-0430

(Dated: 18 November 2003)

Restoration of broken circular symmetry is used to explore the characteristics of the ground states and the excitation spectra of rotating Wigner molecules (RWM's) formed in two-dimensional parabolic N -electron quantum dots. In high magnetic fields, the RWM's are floppy rotors with the energies of the magic angular momentum (L) states obeying $aL + b/L^{1/2}$. Under such fields the ground-state energies (referenced to the kinetic energy in the lowest Landau level) approach the electrostatic energy of N point charges in the classical equilibrium molecular configuration. At zero field and strong interelectron repulsion, the RWM's behave like quasiclassical rigid rotors whose energies vary as L^2 .

PACS numbers: 73.21.La; 71.45.Gm; 71.45.Lr

The belief that the physics of two-dimensional (2D) semiconductor quantum dots (QD's) in high magnetic fields (B) is described [1, 2] by composite-fermions, introduced [3] originally for the bulk fractional quantum Hall effect (FQHE), has been recently challenged [4] by a proposal that the fundamental physical entity in strongly correlated QD's is a *collectively rotating* Wigner (or electron) molecule (RWM or REM). Indeed, it has been lately found that electrons in 2D QD's can undergo in the strongly correlated regime a spontaneous phase transition akin to the Wigner crystallization in the bulk, forming [5, 6, 7, 8] specific polygonal geometric structures that are called Wigner molecules (WM's). These geometric structures break the rotational symmetry (for symmetry restoration, see below) and reflect the presence of many-body crystalline correlations that are revealed, as illustrated previously, in the "humps" of the conditional probabilities [7, 8] and of the broken-symmetry electron densities [5, 6].

The majority of recent studies address the properties of *static* WM's (as a function of the QD parameters) [9, 10, 11, 12]. Here, we study the properties of the *rotating* WM. We show through microscopic many-body investigations that the RWM in high B is a *floppy rotor*, while at large R_W (and zero magnetic field) it transforms into a *rigid rotor*. [The Wigner parameter $R_W \equiv Q/\hbar\omega_0$, where Q is the Coulomb interaction strength; $Q = e^2/(\kappa l_0)$, with $l_0 = \sqrt{\hbar/(m^*\omega_0)}$ being the spatial extent of the lowest single-electron wave function in the external parabolic confinement of frequency ω_0 , and κ is the dielectric constant.] The ability to capture the physics of the electrons in QD's in both the high magnetic field and the field-free regimes is an essential demonstration of the powerful unification offered by the RWM picture, a property not shared by other suggested approaches.

The *collective rotation* of the WM is inherent and natural to the molecular picture. In particular, we show that it is manifested in characteristic energy-vs-

angular-momentum relations for the excitation spectra and in specific limiting values for the ground-state energies. These relations are important in the development of theories of electrons in QD's under the influence of a magnetic-field and in the field-free case, and they can be employed as diagnostic tools for assessing the validity and applicability of alternative theoretical descriptions.

Description of the broad variation of the collective properties of electrons in 2D QD's requires a highly flexible and accurate many-body method. In principle, exact diagonalization (EXD) could have been used; however, its computational limitations are a major obstacle. We demonstrate that the recently proposed [4, 6] two-step method of circular symmetry breaking at the unrestricted Hartree-Fock (UHF) level and of subsequent symmetry restoration via post-Hartree-Fock projection techniques is an accurate and computationally efficient approximation which provides a *unified* microscopic description of the emergent picture of RWM's in 2D QD's.

The restoration of broken circular symmetry is necessary for a proper description of RWM's. Indeed, while the broken symmetry UHF solutions describe *static* WM's [9, 10, 11, 12], it is the symmetry restoration step which describes the rotation of the WM's and underlies the differentiation between rigid and floppy (at high B) rotors.

The two-step method. In general, the localized broken symmetry orbitals are determined numerically via a self-consistent solution of the UHF equations [6]. An efficient alternative, however, is to approximate these orbitals by appropriate analytical expressions [4, 10, 11, 12]. Since we focus here on the second step (restoration of the circular symmetry) and the case of high B , it will be sufficient to approximate the UHF orbitals (first step of our procedure) by (parameter free) displaced Gaussian functions [13]; namely, for an electron localized at Z_j , we use the orbital

$$u(z, Z_j) = \frac{1}{\sqrt{\pi}\lambda} \exp\left(-\frac{|z - Z_j|^2}{2\lambda^2} - i\varphi(z, Z_j; B)\right), \quad (1)$$

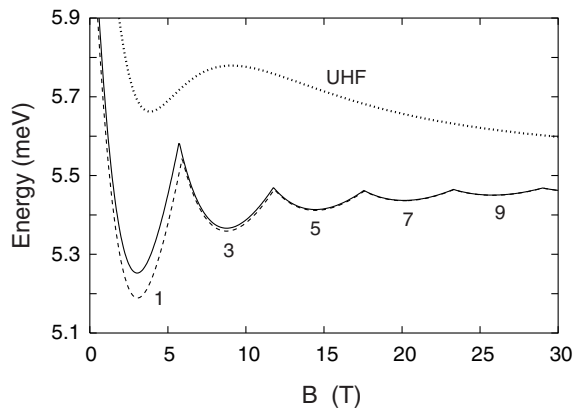


FIG. 1: Total energies, $E - 2\hbar\Omega$, for the triplet state of $N=2$ electrons as a function of the magnetic field B . Solid line: PRJ (rotating WM); dashed line: exact; dotted line: UHF (static WM). The integers below the troughs of the PRJ and exact lines indicate the corresponding magic angular momenta. The parameters are: $m^* = 0.067m_e$, $\hbar\omega_0 = 3$ meV, and $\kappa = 12.9$. Here, as well as in the other figures, the Zeeman contribution is not included, but can be easily added.

with $z = x + iy$, $Z_j = X_j + iY_j$, and $\lambda = \sqrt{\hbar/m^*\Omega}$; $\Omega = \sqrt{\omega_0^2 + \omega_c^2}/4$, where $\omega_c = eB/(m^*c)$ is the cyclotron frequency. The phase guarantees gauge invariance in the presence of a perpendicular magnetic field and is given in the symmetric gauge by $\varphi(z, Z_j; B) = (xY_j - yX_j)/2l_B^2$, with $l_B = \sqrt{\hbar c/eB}$ being the magnetic length. We only consider the case of fully polarized electrons, which is appropriate at high B .

We take the Z_j 's to coincide with the equilibrium positions (forming nested regular polygons [14]) of N classical point charges inside an external parabolic confinement of frequency ω_0 , and proceed to construct the UHF determinant $\Psi^{\text{UHF}}[z]$ out of the orbitals $u(z_i, Z_j)$'s, $i, j = 1, \dots, N$. Correlated many-body states with good total angular momenta L can be extracted [6] from the UHF determinant using projection operators; the projected energies are given by [6]

$$E_{\text{PRJ}}(L) = \int_0^{2\pi} h(\gamma) e^{i\gamma L} d\gamma / \int_0^{2\pi} n(\gamma) e^{i\gamma L} d\gamma, \quad (2)$$

with $h(\gamma) = \langle \Psi^{\text{UHF}}(0) | H | \Psi^{\text{UHF}}(\gamma) \rangle$ and $n(\gamma) = \langle \Psi^{\text{UHF}}(0) | \Psi^{\text{UHF}}(\gamma) \rangle$, where $\Psi^{\text{UHF}}(\gamma)$ is the original UHF determinant rotated by an azimuthal angle γ and H is the many body Hamiltonian (including the vector potential, external confinement, and Coulomb two-body repulsion). We note that the UHF energies are simply given by $E_{\text{UHF}} = h(0)/n(0)$.

Compared to an EXD calculation, the CPU time for calculating the projected energies [see Eq. (2)] increases much slower as a function of L and N . In addition, the computational efficiency of Eq. (2) is greatly enhanced by the knowledge [10] of the analytical forms of the (in general complex) matrix elements of the single-particle

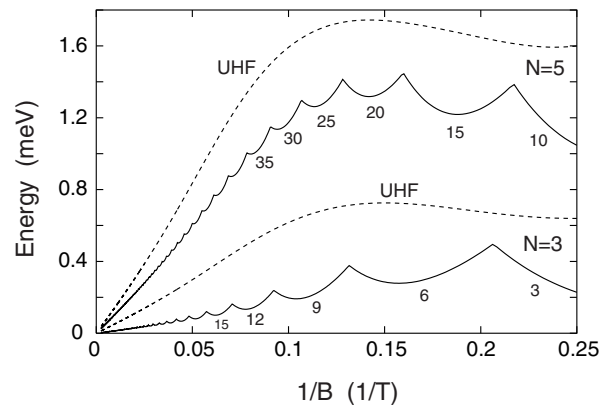


FIG. 2: PRJ (solid lines) and UHF (dashed lines) total energies, $E - N\hbar\Omega$, for the fully spin-polarized ground states of $N = 3$ and $N = 5$ electrons, as a function of $1/B$. The range covered is $4 \text{ T} \leq B \leq 400 \text{ T}$, and the zero of energy corresponds to $E_{\text{cl}}^{\text{st}} = 14.415$ meV for $N = 3$ and to $E_{\text{cl}}^{\text{st}} = 42.873$ meV for $N = 5$. The integers below the troughs of the PRJ curves indicate the corresponding magic angular momenta. The parameters are as in Fig. 1.

and two-body components of H between the displaced Gaussians.

To test the accuracy of our method, we display in Fig. 1 the total energies $E - 2\hbar\Omega$ as a function of the magnetic field for the triplet state of $N = 2$ electrons and for all three levels of calculations, i.e., the UHF, the subsequent projection [PRJ, see Eq. (2)], and the exact result [7]. We observe that the UHF energies fare poorly compared to the PRJ ones; note that for $B > 7$ T, the PRJ and exact results are practically the same. We further note that the UHF energies do not reproduce the characteristic oscillations of the exact ones; these oscillations originate from the fact that only states with magic angular momenta can become ground states (in the case of the triplet state for $N = 2$, the magic angular momenta are $L = 2m + 1$, $m = 0, 1, 2, \dots$).

Ground states at high magnetic field. Fig. 2 displays the ground state energies $E - N\hbar\Omega$ for $N = 3$ and $N = 5$ electrons as a function of $1/B$. Since our method allows us to reach magnetic field values as high as $B = 400$ T, we conclude unequivocally that, as $B \rightarrow \infty$, both the PRJ and UHF energies approach the limiting value corresponding to the classical energy of N point-like electrons at equilibrium [in the $(0, N)$ configuration for $N = 2 - 5$] inside an external parabolic confinement of frequency ω_0 , i.e.,

$$E_{\text{cl}}^{\text{st}}(N) = (3/8)(2R_W)^{2/3} N S_N^{2/3} \hbar\omega_0, \quad (3)$$

with $S_N = \sum_{j=2}^N (\sin[(j-1)\pi/N])^{-1}$ [15]. Except for the $B \rightarrow \infty$ limit, the UHF energies are higher in value than the projected ones.

The projected ground states have magic angular momenta that vary (from one trough to the other) by steps

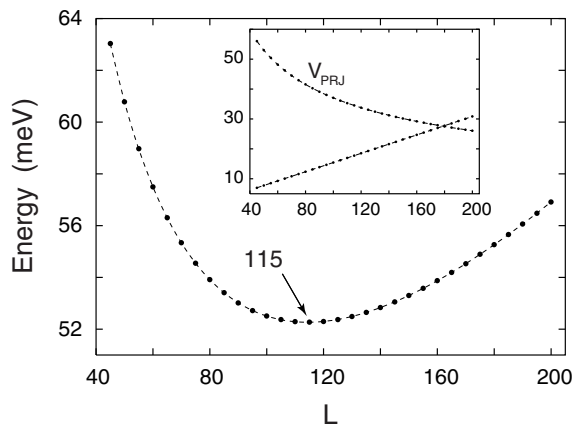


FIG. 3: Projected total energies, $E_{\text{PRJ}} - 5\hbar\Omega$, for the yrast rotational band (states with the lowest energy at magic angular momenta) of $N = 5$ fully-polarized electrons at $B = 60$ T, as a function of the angular momenta L . The ground state has angular momentum $L = 115$. The choice of parameters is: $m^* = 0.067m_e$, $\hbar\omega_0 = 4$ meV, and $\kappa = 12.9$. Inset: The two contributions $E_{\text{PRJ}}^c(L) - 5\hbar\Omega$ and $V_{\text{PRJ}}(L)$ associated with the confinement (lower curve) and the Coulomb interaction (upper curve), respectively.

of N units ($N = 3, 4, 5$) in accordance with the trend found for a much smaller range of angular momenta in earlier EXD studies [8, 17]. With our projection method, we were able to reach remarkably high values of $L = 369, 690$, and 1100 for $N = 3, 4$, and 5 , respectively. The fact that $E_{\text{PRJ}} - N\hbar\Omega$ and $E_{\text{exact}} - N\hbar\Omega$ (see Ref. [16]) tend to $E_{\text{cl}}^{\text{st}}(N)$ for $B \rightarrow \infty$ is a significant finding that has not appeared in the FQHE literature [1, 17]; instead it has been implied that $E - N\hbar\Omega \rightarrow 0$ as $B \rightarrow \infty$. In any case, it is doubtful that the composite-fermion approach can conform to this rigorous limit [16]; indeed the precise value of $E_{\text{cl}}^{\text{st}}(N)$ depends crucially on the long-range character of the Coulomb force acting between localized classical particles, and thus it is a result innate to the WM picture.

Furthermore, this limit points out to interesting experimental ramifications. Namely, at high B , the addition energies (expressed by the finite second difference $\Delta_2 E(N)$), while not conforming to the capacitance–Coulomb blockade model [17], will tend to a constant value $\Delta_{2,\text{cl}}^{\text{st}} E(N) = E_{\text{cl}}^{\text{st}}(N+1) + E_{\text{cl}}^{\text{st}}(N-1) - 2E_{\text{cl}}^{\text{st}}(N)$ (e.g., 3.446 meV for $N = 4$ and the parameters listed in the caption of Fig. 2); this constant value maybe detected experimentally.

The yrast rotational band at high B . The yrast band consists of the lowest energy states (for a given B) having magic angular momenta (the ground state is a member of this band and the remaining states are excited ones). The yrast band for $N = 5$ calculated at $B = 60$ T is displayed in Fig. 3.

The energy of the yrast states is composed [1] of two

TABLE I: Projected interaction energies $V_{\text{PRJ}}(L)$ associated with yrast states at two values of $B = 60$ T and $B \rightarrow \infty$ for $N = 5$ [the (0,5) configuration] and $N = 6$ [the (1,5) configuration], respectively. $f \equiv V_{\text{PRJ}}(L)L^{1/2}/C_V$, where $C_V = 15.388$ for $N = 5$ and $C_V = 18.787$ for $N = 6$. The fractional fillings are calculated through $\nu = N(N-1)/(2L)$. Energies in units of $e^2/\kappa\lambda$ and $e^2/\kappa l_B$ for $B = 60$ T and $B \rightarrow \infty$, respectively. At $B \rightarrow \infty$, $V(L)$ is independent of $\hbar\omega_0$. At large finite B , $V(L)$ depends on $\hbar\omega_0$ through λ .

$N = 5$		$B = 60$ T		$N = 6$		$B \rightarrow \infty$	
$L(\nu)$	V_{PRJ}	f		$L(\nu)$	V_{PRJ}	f	
40(1/4)	2.5000	1.02749		75(1/5)	2.2196	1.02317	
50(1/5)	2.2216	1.02083		135(1/9)	1.6361	1.01186	
60(1/6)	2.0198	1.01669		195(1/13)	1.3561	1.00799	
80(1/8)	1.7409	1.01189		255(1/17)	1.1836	1.00603	
100(1/10)	1.5531	1.00925		315(1/21)	1.0636	1.00484	
120(1/12)	1.4154	1.00757		435(1/29)	0.9039	1.00347	
140(1/14)	1.3089	1.00641		495(1/33)	0.8470	1.00304	
160(1/16)	1.2233	1.00556		555(1/37)	0.7996	1.00271	
180(1/18)	1.1526	1.00491		615(1/41)	0.7594	1.00244	
190(1/19)	1.1216	1.00464		675(1/45)	0.7247	1.00222	

contributions; namely, $E(L) = E^c(L) + V(L)$, where $E^c(L)$ is the confinement energy associated with the external potential (including the kinetic energy), and $V(L)$ is the interaction energy due to the Coulomb force. For high B , it is well known [1, 17] that the confinement energy varies linearly with L ; in particular, $E^c(L) \rightarrow \hbar(\Omega - \omega_c/2)L + N\hbar\Omega$.

We have calculated the projected values [see Eq. (2)] for these two components, namely, $E_{\text{PRJ}}^c(L)$ and $V_{\text{PRJ}}(L)$, for $N = 2 - 6$ and a variety of B values and QD parameters. Our ability to calculate efficiently high L values allowed us to confirm numerically the linear L -dependence of the confinement energy $E^c(L)$, and also the precise proportionality coefficient $\hbar(\Omega - \omega_c/2)$. Moreover, rather unexpectedly, we also find that the interaction energy behaves asymptotically as $L^{-1/2}$, i.e., $V(L) \rightarrow C_V/L^{1/2}$, where C_V is a constant given below.

TABLE I lists $V_{\text{PRJ}}(L)$ for $N = 5$ and $B = 60$ T, as well as for $N = 6$ [the (1,5) configuration] and $B \rightarrow \infty$; the latter limit can be easily taken by setting [4] $\lambda = l_B\sqrt{2}$ in Eq (1), which restricts the electrons to the lowest Landau level. From TABLE I, one can see that the quantity $f \equiv V_{\text{PRJ}}(L)L^{1/2}/C_V$ approaches unity as the angular momentum increases, where $C_V = K^{3/2}(S_K/4 + \delta_{K,N-1})e^2/(\kappa\lambda)$, with $K = N$ or $N - 1$ for WM's in the (0, N) or (1, $N - 1$) configurations, respectively.

The $C_V/L^{1/2}$ asymptotic dependence of the interaction energy can be readily associated with a model [8] of a classical *floppy molecule* rotating inside a parabolic confinement characterized by a frequency Ω [18]. Indeed, the energy of such a molecule is given by

$$E_{\text{cl}}^{\text{rot}}(K) = \hbar^2 L^2 / (2\mathcal{J}(a)) + \mathcal{J}(a)\Omega^2 / 2 - \hbar\omega_c L / 2 + K(S_K/4 + \delta_{K,N-1})e^2/(\kappa a), \quad (4)$$

TABLE II: Projected total energies $E_{\text{PRJ}}(L)$ at $B = 0$ and $R_W = 200$ associated with yrast states for $N = 5$ electrons [(0,5) configuration]. $\tilde{f} \equiv C_R/C_R^{\text{cl}}$ (see text). Energies in units of $\hbar\omega_0$.

L	E_{PRJ}	\tilde{f}	L	E_{PRJ}	\tilde{f}
0	323.3070		25	324.7657	0.988
5	323.3656	0.992	30	325.4033	0.986
10	323.5414	0.992	35	326.1537	0.983
15	323.8338	0.991	40	327.0153	0.981
20	324.2422	0.989	45	327.9866	0.978

where $\mathcal{J}(a) = Km^*a^2$ is the moment of inertia of K point-like electrons located at the vertices of a regular polygon of radius a . The second term is the potential energy due to the confinement, and the last term is the classical Coulomb-repulsion electrostatic energy. At given B , the radius of this floppy molecule varies with L , and for large angular momentum (and/or high B) it is given by $a \approx \lambda\sqrt{L/K}$ [$a \rightarrow \sqrt{2\hbar cL/(eBK)}$ for $B \rightarrow \infty$]. Substitution into Eq. (4) yields the aforementioned linear and $1/L^{1/2}$ contributions, i.e.,

$$E_{\text{cl}}^{\text{rot}}(K) \approx \hbar(\Omega - \omega_c/2)L + C_V/L^{1/2}. \quad (5)$$

A semiclassical approximation $L_{\text{gs}}^{\text{cl}}$ of the ground-state angular momentum minimizes Eq. (5), yielding $L_{\text{gs}}^{\text{cl}} \propto B$. Consequently, the ground-state radius $a_{\text{gs}} \rightarrow r_0$ as $B \rightarrow \infty$, where $r_0 = l_0 R_W^{1/3} (S_K/4 + \delta_{K,N-1})^{1/3}$ is the radius of the *static* classical Wigner molecule. Note that, in the ground state as B increases, the WM rotates faster in order to maintain the requisite value of $a_{\text{gs}} = r_0$.

We note that this inverse-square-root-of- L law at constant B for the Coulomb interaction energy has also been overlooked in the FQHE literature [1, 17]. This law provides a nontrivial test in that it lends further support to the RWM picture; especially since it also applies in the $B \rightarrow \infty$ limit (see right part of TABLE I), which restricts the electrons to the lowest Landau level (FQHE regime). We note that high L 's correspond to lower fractional fillings, experimentally achievable in high-mobility samples.

The rigid rotor at zero magnetic field. At $B = 0$, we found it advantageous to allow the width λ and the positions Z_j 's of the displaced Gaussians to vary in order to minimize (for each L) the projected energy [Eq. (2)]. For large R_W 's and for $N = 2 - 5$ electrons, we find that the energies of the states in the yrast band can be approximated by

$$E_{\text{PRJ}}(L) \approx E_{\text{PRJ}}(0) + C_R L^2, \quad (6)$$

where the rigid-rotor coefficient C_R is essentially a constant whose value is very close (see the \tilde{f} values) to the classical one, corresponding to point charges in their $(0, N)$ equilibrium configuration inside a parabolic confinement of frequency ω_0 ; i.e., $C_R \approx C_R^{\text{cl}} = \hbar^2/(2\mathcal{J}(r_0))$.

In Table II, we list calculated $E_{\text{PRJ}}(L)$ values for $N = 5$ when $R_W = 200$. The fact that $\tilde{f} \equiv C_R/C_R^{\text{cl}} \approx 1$ for $L \leq 45$ illustrates that the RWM behaves as a quasi-classical rigid rotor. For smaller values of R_W , the rigidity of the RWM is progressively reduced [7]. We note that $E_{\text{PRJ}}(0) - N\hbar\omega_0$ is very close to the classical electrostatic value given by Eq. (3).

Conclusions. Using the method of restoration of broken circular symmetry, we have shown that the RWM's in QD's exhibit characteristic properties as a result of their collective rotation: (I) in high B , they behave like *floppy rotors* and the energies of the magic states in the lowest rotational (yrast) band, associated with magic angular momenta, obey $aL + b/L^{1/2}$. In addition, the ground-state energies (referenced to the kinetic energy in the lowest Landau level) approach the limit of the electrostatic energy of N point charges in their classical equilibrium molecular configuration; (II) at $B = 0$ and strong interelectron repulsion, the RWM's behave like *quasiclassical rigid rotors* whose yrast band exhibits an L^2 -dependence. The rotating-Wigner-molecule picture unifies the description of the various physical regimes of strongly correlated electrons in 2D QD's. This unification is achieved through the computationally powerful method of restoration of broken symmetries via projection techniques.

This research is supported by the U.S. D.O.E. (Grant No. FG05-86ER45234).

-
- [1] J.K. Jain and T. Kawamura, Europhys. Lett. **29**, 321 (1995).
 - [2] A.L. Jacak, P. Hawrylak, and A. Wojs, *Quantum Dots* (Springer, Berlin, 1998), in particular Ch. 4.5.
 - [3] J.K. Jain, Phys. Rev. B **41**, 7653 (1990).
 - [4] C. Yannouleas and U. Landman, Phys. Rev. B **66**, 115315 (2002); **68**, 035326 (2003).
 - [5] C. Yannouleas and U. Landman, Phys. Rev. Lett. **82**, 5325 (1999); Phys. Rev. B **61**, 15 895 (2000).
 - [6] C. Yannouleas and U. Landman, J. Phys.: Condens. Matter **14**, L591 (2002); Phys. Rev. B **68**, 035325 (2003).
 - [7] C. Yannouleas and U. Landman, Phys. Rev. Lett. **85**, 1726 (2000).
 - [8] P.A. Maksym, Phys. Rev. B **53**, 10 871 (1996).
 - [9] B. Reusch, W. Häusler, and H. Grabert, Phys. Rev. B **63**, 113313 (2001).
 - [10] J. Kainz, S.A. Mikhailov, A. Wensauer, and U. Rössler, Phys. Rev. B **65**, 115305 (2002).
 - [11] P.A. Sundqvist, S.Yu. Volkov, Yu.E. Lozovik, and M. Willander, Phys. Rev. B **66**, 075335 (2002).
 - [12] B. Szafran, S. Bednarek, and J. Adamowski, J. Phys.: Condens. Matter **15**, 4189 (2003).
 - [13] For the use of Gaussians with variational parameters, see the case of $B = 0$ below.
 - [14] $(0, N)$ denotes a single regular polygon with N vertices; $(1, N - 1)$ denotes a regular polygon with $N - 1$ vertices and one electron at the center.

- [15] For the same parameters as those in Fig. 2, we have also calculated the ground-state energies $E_{\text{PRJ}} - 4\hbar\Omega$ for $N = 4$ electrons in the range $4 \text{ T} \leq B \leq 400 \text{ T}$, and found that they converge to $E_{\text{cl}}^{\text{st}}(4) = 26.921 \text{ meV}$.
- [16] For the exact ground-state energy, this is a rigorous mathematical result; see J. Yngvason, math-ph/9812009 and E.H. Lieb, J.Ph. Solovej, and J. Yngvason, Phys. Rev. B **51**, 10 646 (1995).
- [17] S.R.E. Yang, A.H. MacDonald, and M.D. Johnson, Phys. Rev. Lett. **71**, 3194 (1993).
- [18] Note the capital Ω . The low B value (20 T) and limited L range ($\lesssim 50$) of the EXD calculations of Ref. [8], however, did not offer convincing evidence regarding the relevance of this classical-rotating-molecule model for QD's in high B , see, e.g., Ref. [2] and S.M. Reimann and M. Manninen, Rev. Mod. Phys. **74**, 1283 (2002).